

EXPERIMENTAL AND NUMERICAL INVESTIGATIONS OF A SWIRL-STABILIZED JET ENGINE COMBUSTOR

Bora O. Cakir¹, David Sanned², Pierre Vauquelin³, Megha Prakash², Jan-Peter Hannappel¹, Arman Subash⁴, Mattias Richter², Xue-Song Bai³, Christer Fureby¹

¹Division of Heat Transfer, Department of Energy Sciences, Lund University, Sweden
²Division of Combustion Physics, Department of Physics, Lund University, Sweden
³Division of Fluid Mechanics, Department of Energy Sciences, Lund University, Sweden
⁴Lund University School of Aviation, Lund University, Sweden

Corresponding author: Bora O. Cakir (bora.cakir@energy.lth.se)

Abstract

Sustainability of future aviation platforms is heavily dependent on the lower emission capabilities of aeroengines which can be addressed by means of utilizing jet fuels of biological origin. Thus, an extensive experimental and numerical investigation campaign utilizing the Triple Annular Research Swirler (TARS) burner is started to understand the thermochemical properties and combustion characteristics of these fuels. The experiments are performed in atmospheric conditions with the TARS burner operated under various configurations of fuel injection, swirler combination and boundary conditions using methane and ethanol for gaseous and liquid fuel sources respectively. Preliminary results of the commissioning campaign for the liquid fuel operation of TARS burner integrated to atmospheric combustion rig are provided via chemiluminescence images. Moreover, the numerical investigations are conducted via Large Eddy Simulations in which kerosene-based (Jet A) and biograde (ATJ C1) jet fuels are used. The simulation results performed using operating conditions which will be targeted at the later stages of the experiments are analyzed to serve as a precursor to future measurements.

Keywords: Sustainable aviation, biofuels, jet engine, swirl-stabilized combustion, TARS

1. Introduction

Increasing requirements on emission regulations for a sustainable and cleaner future aviation platform demand new fuels and advanced combustion technologies for sustainable aeroengines. In this regard, the recent advancements in hydrogen utilization technology revealed a possible path for lower emissions and higher efficiency of propulsion systems. Nonetheless, the use of hydrogen requires substantial changes to the conceptual design of the aeroengines, structural components of the airframes, and a significant modification of infrastructure to accommodate the widespread use [1]. As an alternative solution, the use and production of bio-jet fuels has proven to be an effective solution. The wide variety of feedstock utilization, various pathways for production, similar storage behavior to kerosene-based jet fuels, and the minimal requirements for modifications to actively employed aeroengines increased the popularity of using sustainable aviation fuels with a biological origin [2]. However, the differences in injection, combustion and emission characteristics demand proper characterization of fuels for understanding the necessary design changes as well as the short- and long-term consequences of utilizing each fuel composition [3, 4].

In this regard, a swirl burner that mimics the combustors of aeroengines, referred to as the Triple Annular Research Swirler (TARS) burner, is utilized for the characterization of flame interactions with turbulent swirling flows for various swirl configurations, fuels, injection strategies and operating conditions. The TARS burner has been employed previously to investigate both non-reactive and reactive flow dynamics in open and confined combustion chamber conditions [5]. These studies include vortex breakdown and positioning in non-reactive flow scenarios [6], stability of swirling flame via proper orthogonal decomposition [7], characterization of fuel injection with varying multi-swirler arrangements [8], breakdown of vortical structures in the swirling flow [9], dynamics of lean blow out

[10], and lean direct-injection [11] mechanisms, which are especially relevant for reducing flame temperatures and emissions. Whilst most of the aforementioned work is performed experimentally, there are numerical studies as well performed on the TARS geometry. Grinstein *et al.* [12] performed Large Eddy Simulations (LES) with a hybrid approach using the data from Reynolds-averaged Navier-Stokes (RANS) simulations and experimental campaigns for the setting of boundary conditions while the LES enabled detailed characterization of the unsteady non-reactive swirling flow downstream of the burner. Fureby *et al.* [13] analyzed the dynamical interactions between the turbulent flow and flames on TARS, which in combination with the experimental campaigns provided a detailed description of the lean direct fuel injection (LDI) process in multi-swirl gas turbine combustors. Finally, ludiciani *et al.* [14] investigated the flow behavior inside the burner by means of LES, for which the flow inside the burner is not accessible in the case of experiments.

In line with the previous work utilizing the burner arrangement for studying relevant flow structures and flame behavior in aero engine combustors, the current work aims to characterize the swirl-stabilized flame behavior and commission the TARS burner for investigation of direct lean fuel injection, flow and flame interaction, and combustion characteristics of the various bio jet fuels. While the gaseous fuel operation is utilized as a precursor in unconfined conditions, liquid fuel tests with ethanol allow the characterization of burner behavior under LDI for both unconfined and confined combustion analysis. Numerical simulations based on Finite Rate Chemistry LES (FRC-LES) will be used in parallel to experimental investigations to characterize the TARS burner, and in particular, how different bio-jet fuels behaves compared to classical fossil jet fuels such as Jet A and JP5.

2. Methodology

2.1 Triple Annular Research Swirler (TARS)

The TARS fuel injector was developed by Delavan Gas Turbine Products, a division of Goodrich Corporation, in collaboration with General Electric Aircraft Engines. The TARS is equipped with three concentric swirlers with various vane angles: the two inner ones are axial while the outer is a radial swirler, see Fig.1. The outer diameter of the radial swirler is D = 5.08 mm, which is used in the following as a reference for non-dimensional coordinates.

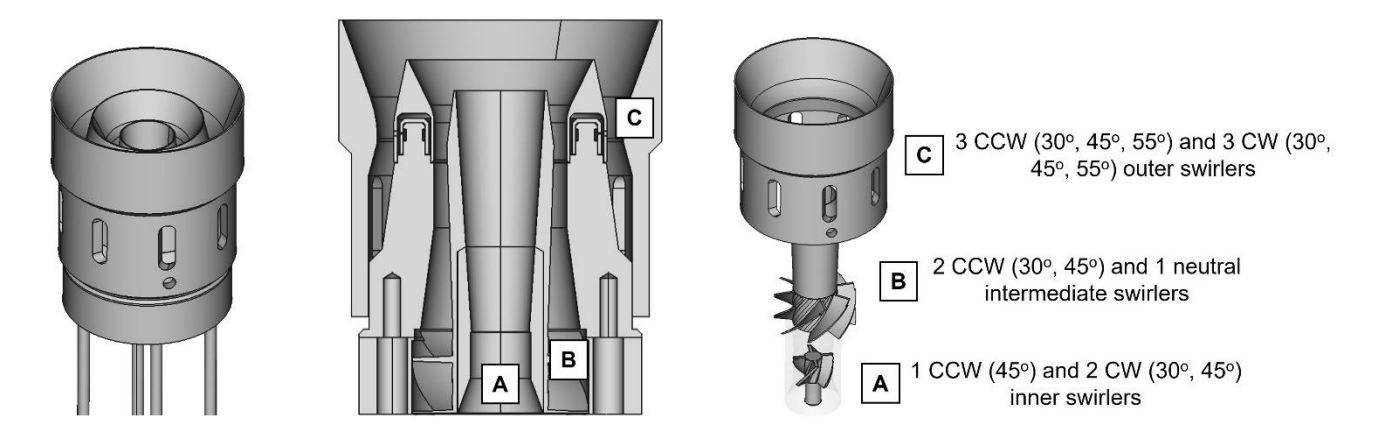


Figure 1 – Triple Annular Research Swirler (TARS) burner with three swirlers: inner(A), intermediate(B) and outer(C).

TARS burner has an inventory of large number of swirlers with various intensities and flow directions throughout the three swirling channels. This, in combination with the modular structure of the burner, allows for a detailed investigation of interactions between swirling turbulent flows and non-premixed flames. The burner has fuel outlets in both outer and intermediate swirl channels with 8 holes (referred to as the main fuel outlet) and 4 holes (referred to as the pilot fuel outlet) respectively. The burner has two plenums separately for the pilot and main fuel supply which are connected to individual supply lines. This enables different configurations in terms of pilot and main fuel selection to be performed. Accordingly, for the liquid operation the pilot injection is fed with methane while liquid fuel is supplied to the main injection holes.

2.2 The Experimental Setup

The experiments were performed in an atmospheric combustion rig, consisting of an inlet flange, a flow conditioning chamber (0.61 m, long) and a plenum chamber (0.36 m, long). The TARS is centered on a mounting plate at the end of the plenum chamber. Upstream the swirlers, the flow passes through two turbulence grids. The outer swirler is flush mounted on the upper surface of the plate. The flow downstream of the burner is confined within a purpose-built combustion chamber. The 400 mm long chamber has a quadratic 140×140 mm cross-section and 4-way optical access through quartz windows to allow non-intrusive diagnostics to be conducted. The chamber is followed by an exhaust placed ~1 m downstream of the burner to avoid exhaust gases being dispersed in the laboratory. The atmospheric rig is equipped with optical diagnosis techniques for the determination of flow/flame characteristics. These include CH* and C2 chemiluminescence (visible spectrum) imaging utilized in the current investigations for which Basler Ace acA1920-40gm and Photron FASTCAM SA-Z high-speed cameras are used.



Figure 2 – Atmospheric combustion rig of Lund University, Division of Combustion Physics and integrated TARS burner.

2.3 The Numerical Setup

The unsteady reactive flow simulations are carried out using the open-source OpenFOAM® C++ library [15], and the simulation set-up is described in the following section. Figure 3 shows the configuration of the TARS burner, the computational domain, and the associated mesh grid used to perform the reactive Large Eddy Simulations. The geometry used for the numerical investigations implies the co-rotating configuration with both outer and intermediate swirlers assembled with 8 vanes each at an angle of 45° in a counterclockwise orientation. The inner swirler is composed of 4 vanes at 55°, also in CCW orientation. Upstream of the TARS burner, the settling chamber is modeled by a cylindrical plenum whose diameter is dplenum=134 mm. It is assumed in the current study that the turbulent flow structures, developed upstream in the settling chamber, mainly break when the flow reaches the swirler entries, which affects the downstream flow field. The uniform inlet velocity is determined by specifying the ambient air mass flow rate, equal to 34 g/s for the operated design conditions. With such mass flow rates, at room temperature of 20°C and atmospheric pressure, the Reynolds number at the TARS nozzle is estimated to be Re_D≈50,000. As in the experimental setup, the nozzle of the TARS burner is flush mounted within the quadratic confinement chamber, 400 mm long, with a section of 140 mm x 140 mm. The convergent quadratic-to-circular pipe at the outlet of the domain is also considered for the simulations. At this point, the outlet patch is handled using a wave-transmissive pressure condition [16] to avoid pressure reflections. A no-slip condition is applied to all walls in the domain. For the plenum upstream of the burner and for TARS itself, the thermal condition is assumed to be adiabatic. For the bottom wall (dome) surrounding the TARS nozzle, a fixed temperature of 800 K is applied, as of estimation prior to experiments. For the rest of the confinement chamber, different patches are defined in the setup to differentiate the quartz windows from the steel walls and apply different thermal conductivity coefficients using the "externalWallHeatFluxTemperature" boundary condition in OpenFOAM. Regarding the global fuel-toair ratio, the preliminary study is focused on the stoichiometric conditions: global equivalence ratio ϕ =1, for both Jet A and an Alcohol to Jet (ATJ) fuel referred to as C1 [17]. The computational setup employs an unstructured grid composed of 12 million tetrahedral cells. For all simulations, the Courant number is kept below 0.8.

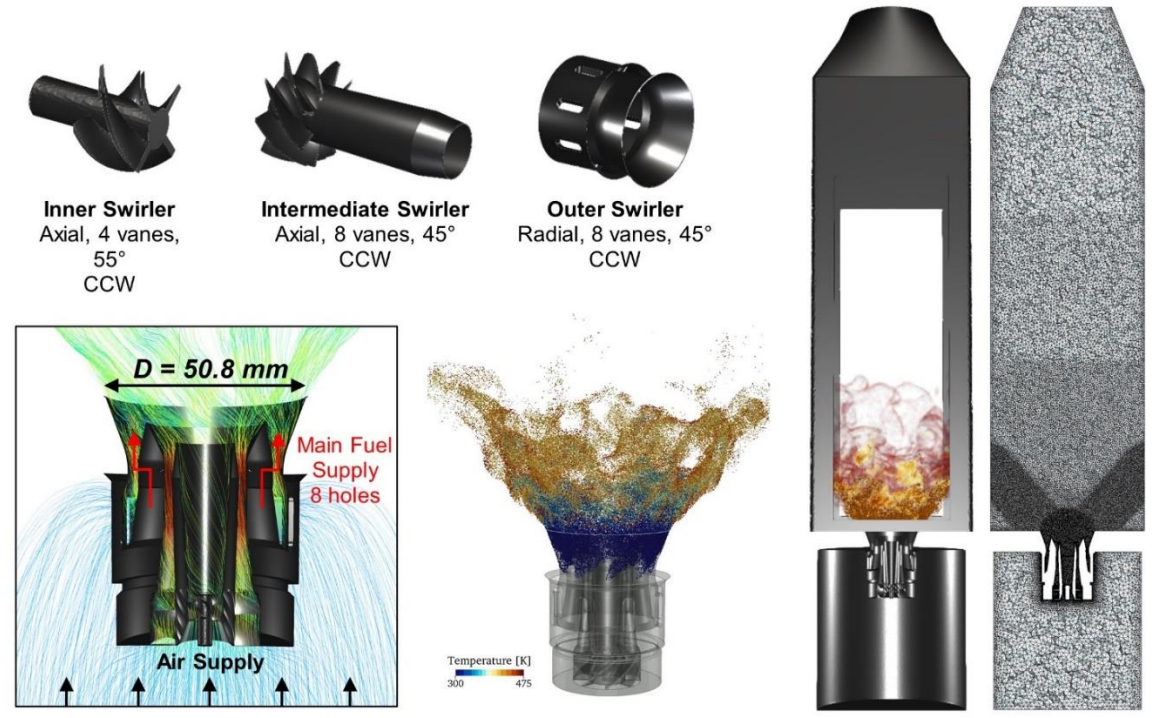


Figure 3 – CAD model of the TARS burner components (top left), clip of the assembled TARS burner with velocity streamlines (bottom left), glyph of the Lagrangian spray cloud obtained for Jet A coloured with temperature (bottom middle), CFD model of the TARS mounted in the confinement chamber, along with the spray cloud, evaporated fuel and a 3D rendering of the heat release, and the computational mesh grid (right).

The reactive LES model uses spatially filtered, unsteady, compressible flow transport equations for mass, momentum, energy, and chemical species mass fractions. The governing equations are closed using the thermal state equation for an ideal gas, with Fourier heat conduction and Fickian diffusion [18]. The Prandtl and Schmidt numbers are assumed to be constant, and the Localized Dynamic kequation Model [19] is used to solve the sub-grid scale interactions. Arrhenius rate laws allow computing the chemical reaction rates, giving out net production rates for each individual species according to the law of mass-action. To compute the reaction rate and model the interaction with the turbulent flow, the Partially Stirred Reactor Reactor (PaSR) model is used [20], assuming that real flames are much thinner than any computational cell. Thus, reaction occurs in a localized thin structure immersed in a non-reacting zone, and the division of the computational cell is based on the comparison between the chemical and turbulent time scales. For simplicity it is assumed that the fuel is fully atomized at its injection from the eight holes in the outer swirler channel, where the Lagrangian particles are injected (each particle representing a group of fuel droplets). The present study targets category A jet fuel: A2, representing Jet A, whose average formula is C₁₁H₂₂, and a category C fuel, C1, whose average formula is C₁₃H₂₈. The alternative fuel C1 is a neat alcohol-to-jet biofuel and is notable for its very low aromatics content and Cetane Number (CN) compared to conventional jet fuels. For both Jet A and ATJ C1, the recently developed "Z79" class of reduced reaction mechanisms is used [21], consisting of 31 species and 79 reactions.

3. Results

3.1 Experimental Results

The experimental campaign performed to commission the TARS burner and investigate the combustion behavior of non-premixed liquid fuels is initiated with unconfined conditions. This provides the first set of analysis which is aimed to match the operating and boundary conditions previously employed by Gutmark et al. [5]. For the current investigation, two swirler configurations are utilized;

no inner, CCW 45° intermediate, CCW 45° outer and CW 30° inner, CCW 45° intermediate, CCW 45° outer. These configurations are determined in accordance with operability tests performed prior to the commissioning campaign. Throughout the preliminary tests, the burner assembly and the atmospheric rig have undergone a series of modifications to improve cold flow uniformity, fuel injection distribution and fuel/air mixing quality. In this regard, the burner assembly is cleaned via multiple stages of ultrasound bathing to ensure the liquid fuel supply plenum and injection holes are free of residual particles (i.e., flow and/or fuel tracers). The burner settling chamber is fitted with a honeycomb flow conditioner to reduce transverse motion and corner flow effects within the settling chamber. The fuel supply system of the atmospheric rig is reconfigured to streamline the combined operation with a simultaneous supply of gaseous and liquid fuels. Finally, the mass flow meters that measure the air mass flow rate supplied by the blower are calibrated to validate the accurate control of operating conditions.

3.1.1 Non-reactive flow behavior

Prior to the reactive flow experiments, cold flow characterization is performed by means of temperature measurements using a thermocouple and a cross-axis transverse system (Fig.4, left). First, a cross-axis measurement along two perpendicular coplanar lines over the transverse plane located 1.5mm downstream of the TARS burner exit is performed Accordingly the results provided in Fig.4 (middle) confirmed the flow uniformity along the azimuthal axis over the burner exit in terms of temperature. Moreover, a second measurement is performed to map the spatial temperature distribution over a quadrant of the transverse plane at the same longitudinal location. The corresponding temperature map illustrated in Fig.4 (right) clearly shows excellent flow uniformity along a larger portion of the azimuthal coordinate system.

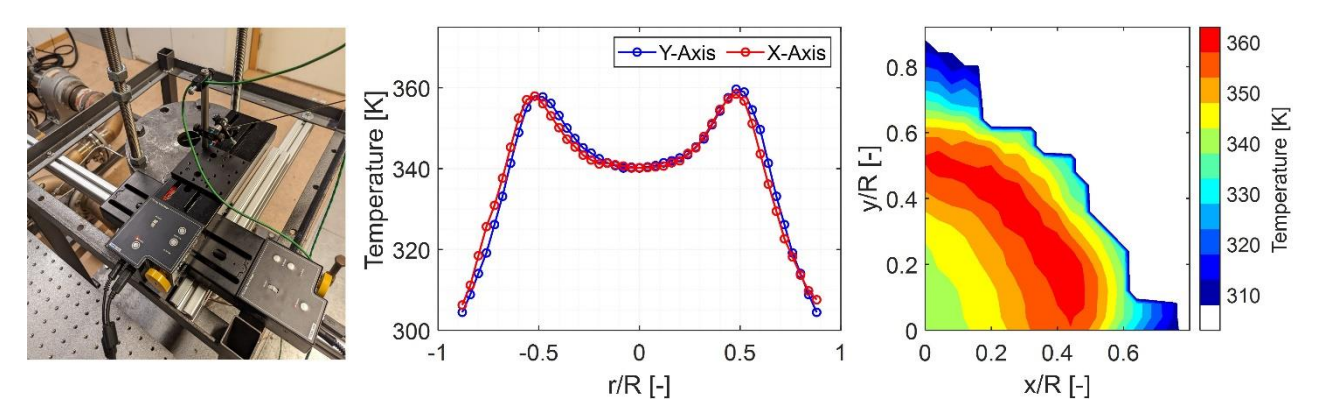


Figure 4 – Cross-axis transverse system with thermocouple for temperature mapping (left). Temperature distribution over the exit plane of the burner at z=1.5mm (middle and right).

3.1.2 Unconfined gaseous fuel operation

The first set of reactive flow experiments is performed using methane (CH₄) as the gaseous fuel source injected from the main fuel injection holes. During the tests, the fuel/air ratio is adjusted to keep the mixture at stochiometric conditions (ϕ =1). For the gaseous fuel tests, the swirler configuration with no inner swirler was selected due to prior tests denoting pure radial exit flow behavior is at high mass flow rates of air. This prevented the desired operating conditions at higher Re_D values and thermal load settings to be achieved. The results provided in Fig.5 demonstrate instantaneous and time-averaged chemiluminescence imaging within the visible spectrum. Hence, the signal intensity captured mainly represents the luminosity received from the CH* and C₂ signal intensity which is heavily correlated with the local heat release. For the measurements, a range of Re_D between $7 \times 10^3 \le Re_D \le 16 \times 10^3$ is investigated. Thus, maintaining the stochiometric conditions, higher Re are achieved by simultaneously increasing the air and fuel mass flow rates which also means that the thermal load varies within a range of 15 kW to 25 kW.

Overall, a symmetric flame behavior can be observed over the range of testing conditions. With the increasing thermal load and Reynolds number, the flame lifts off from the burner nozzle and the total volume of the reaction zone increases (Fig.5, 3rd and 4th columns). Due to the absence of an inner

swirler, a large ratio of the air mass flow rate is directed toward the inner channel of the burner which results in a strong core flow with high axial momentum. This yields a low MFR delivered to the outer radial swirler, which in turn reduces the azimuthal momentum and intensity of the swirl and prevents the occurrence of a vortex breakdown. Thus, the absence of vortex breakdown prevents the generation of a swirl-stabilized flame. As the thermal load increases, the axial momentum of the airflow exiting the TARS burner also increases which reduces the influence of the radial swirler leading to an increasingly skewed flame (Fig.5, 4th column).

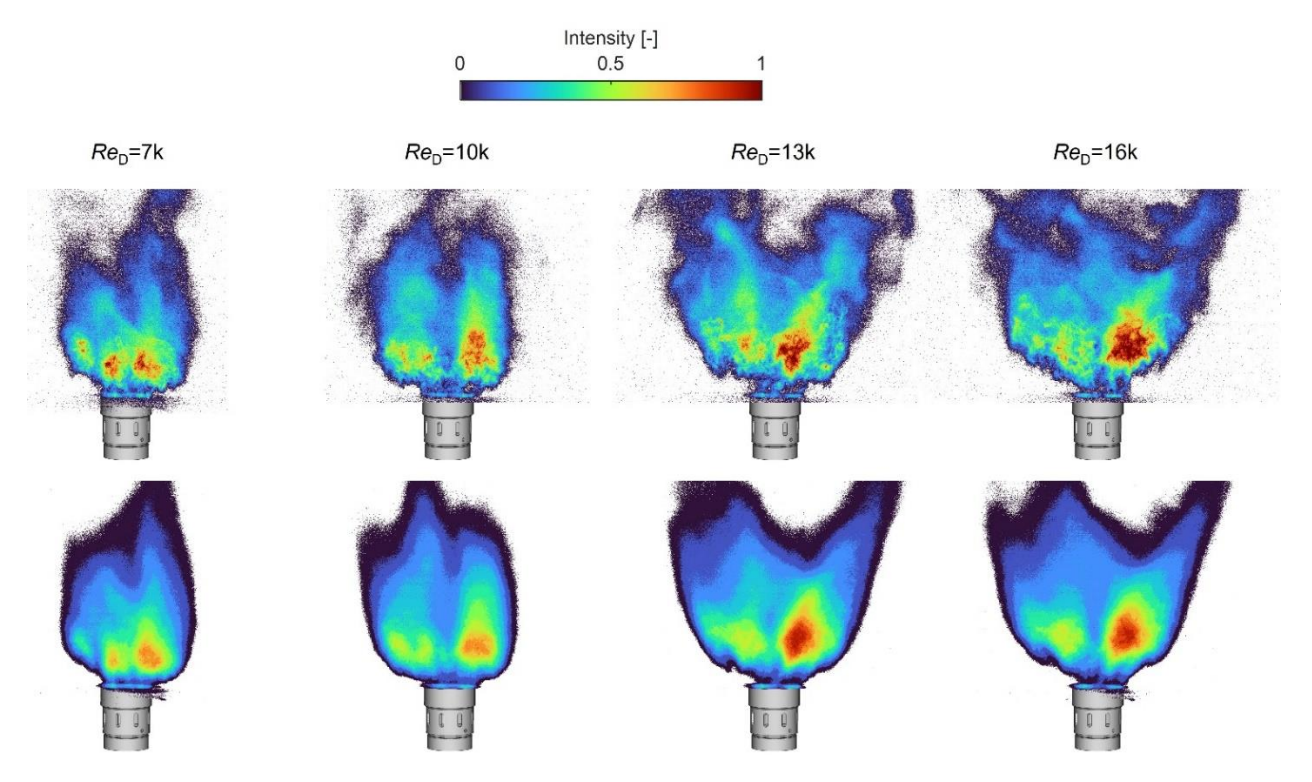


Figure 5 – Instantaneous (top) and time-averaged (bottom) chemiluminescence images for methane/air combustion at various Reynolds numbers; $Re_D = 7 \times 10^3$ (1st column), $Re_D = 10 \times 10^3$ (2nd column), $Re_D = 13 \times 10^3$ (3rd column) and $Re_D = 16 \times 10^3$ (4th column).

3.1.3 Unconfined liquid fuel operation

Commissioning of the liquid fuel operation of the TARS burner is underway, with the initial fuel investigated being ethanol, which will also serve to set a reference case. Testing is initiated with the same swirler configuration that was utilized for the methane cases shown in Fig.5; thus, no inner swirler is mounted in the burner at the beginning. The corresponding flame behavior was observed to be heavily affected by the insufficient air entrainment into the radial swirler channel where the main (liquid) fuel injection holes are located. This leads to multiple issues with liquid fuel operation. First of all, due to the low speed and momentum of the airflow inside the outer swirler channel, the liquid flow injected into the crossflow is not atomized properly. Hence, the droplet breakdown is not strong, keeping the size of the droplets large, which hinders the evaporation process. Moreover, due to the low momentum of air inside the channel, the drag force exerted on the particles is also small, leading to a significant amount of fuel not being carried to the reaction zone. Therefore, when combined with the absence of a strong swirling flow, the improper evaporation and insufficient mixing intensity, a uniform distribution of fuel/air mixture within the reaction zone could not be reached (Fig.6, A). Thereafter, in order to improve flow uniformity and flame symmetry, the mass flow rate ratio is aimed to favor the outer swirler, which would increase the swirl intensity and azimuthal momentum of the air exiting the TARS burner. To do so, a counter-rotating (CW) low-intensity (30°) inner swirler is mounted in the burner assembly.

Owing to the increased MFR ratio to the outer radial swirler, the azimuthal momentum is amplified substantially promoting vortex breakdown and leading to the swirl stabilized flame. Moreover, the alleviated axial momentum due to the low mass flow rate ratio entrained into the inner channel,

increases the residence time of the fuel/air mixture in proximity to the reaction zone, which contributes to considerably enhanced mixing characteristics. As a result, a significantly improved flame symmetry is confirmed with chemiluminescence imaging acquired from multiple phase angles over the line of sight perpendicular to the burner longitudinal axis for air mass flow rates higher than 20g/s ($Re_D \sim 30k$). (Fig.6, B and Fig.7).

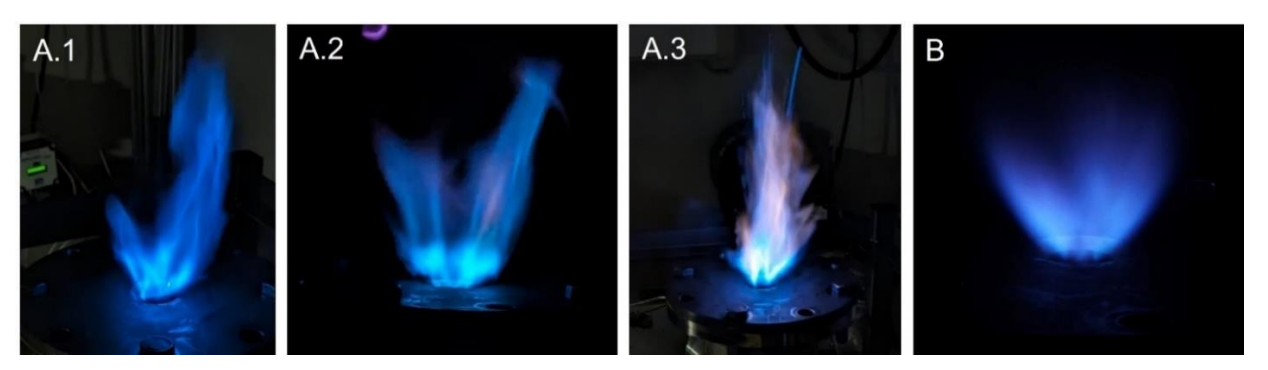


Figure 6 – Chemiluminescence photos of ethanol/air combustion with pilot methane support for no inner swirler (A) and 30° CW inner swirler (B).

During the liquid fuel tests with a 30° CW inner swirler, the operating conditions at Re_D~40k and ~70kW are reached while a global equivalence ratio of ϕ =1 is aimed to be maintained. However, due to the tests being performed without a combustion chamber (unconfined), significant air entrainment and fuel spillage are observed to cause leaner burning conditions compared to stoichiometry. Furthermore, in order to ensure operability at elevated Reynolds numbers and improve the lean blowoff limits, the air temperature is increased to 420 K at the settling chamber, increasing the temperature at the exit of the burner. Since the mass flow rate of air is aimed to be maintained, the axial velocity is required to be increased in order to match the reduction in density of air. Thus, the axial momentum of the air leaving the burner increased, which reduces the residence time of the fuel/air mixture. Moreover, a reduction of air temperature at a constant mass flow rate results in a decreasing Reynolds number due to the higher viscosity of air at elevated temperatures. This indicates a lower mixing intensity of heated air and injected fuel. Therefore, a significant part of the evaporated fuel gets ejected before it can be completely mixed and reacted. On the contrary, the increase in axial velocity affects the Weber number, leading to an amplified break-up of liquid droplets. The increased surface area to volume ratio enhances heat transfer between the heated air and liquid droplets, promoting earlier evaporation of fuel. Thus, the corresponding residence time of fuel in the gaseous phase in proximity to the reaction zone increases, which would contribute to improved mixing of fuel with the air prior to combustion. The balance between these two processes will be investigated during confined measurements utilizing a combustion chamber.

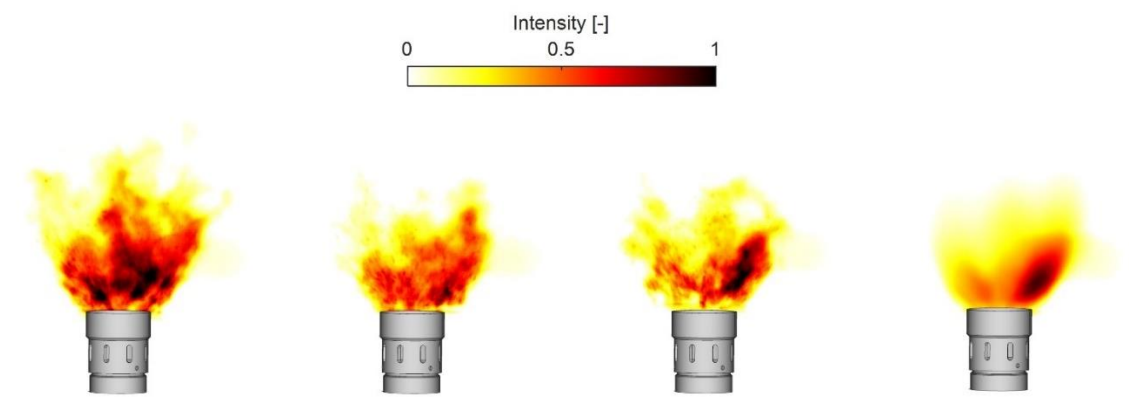


Figure 7 – Instantaneous (1st to 3rd columns) and time-averaged (4th column) chemiluminescence images of unconfined ethanol/air combustion at $Re_D = 22 \times 10^3$ and $\phi = 1$ with pilot methane support using a 30° CW inner swirler.

3.1.4 Confined liquid fuel operation

Following the unconfined experiments with liquid fuel operation, tests with optical confinement are

initiated. The procedure for the confined tests starts with an ignition using only the pilot methane flame to generate a small-scale, non-premixed flame. Then, the optical confinement is placed, and liquid fuel injection is started. During the confined experiments, the air temperature at the settling chamber was set to 450 K to maximize liquid fuel evaporation upon injection and to prevent flame attachment to the optical confinement walls.

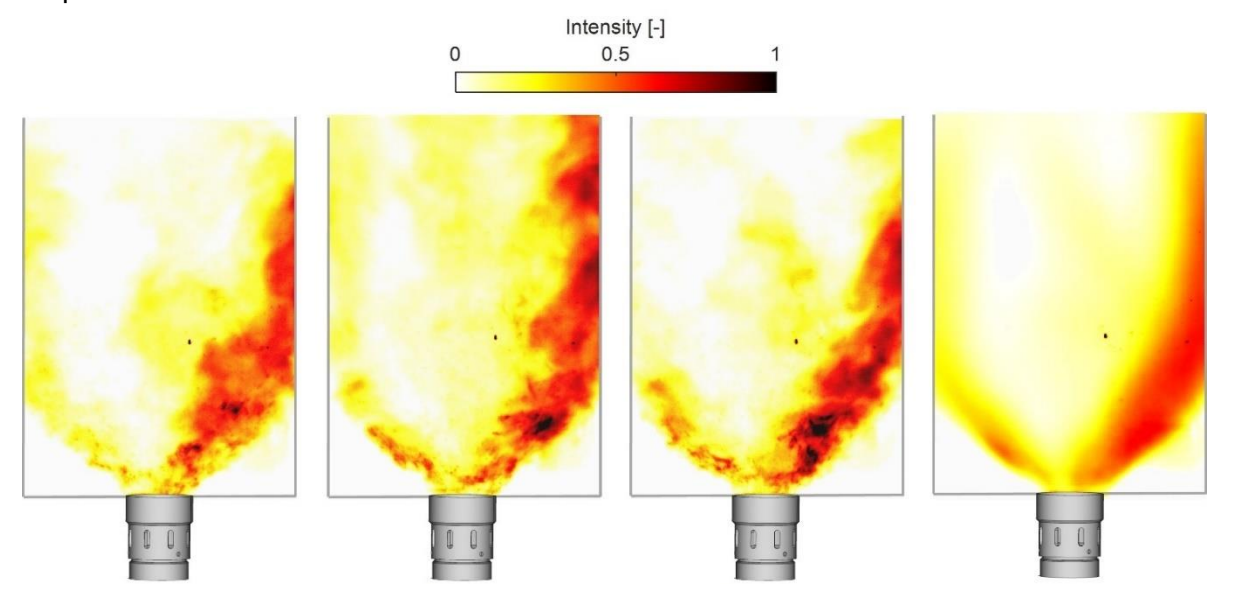


Figure 8 – Instantaneous (1st to 3rd columns) and time-averaged (4th column) chemiluminescence images of confined ethanol/air combustion at $Re_D = 17 \times 10^3$ and $\phi = 0.9$ with pilot methane support using a 30° CW inner swirler.

As the thermal load and Reynolds number are increased by increasing the air and ethanol mass flow rates, a relatively constant equivalence ratio (ϕ =0.9) is aimed, and the pilot methane support is kept at a constant mass flow rate. This process is referred to as the "ramp-up," during which the flame dynamics vary significantly. These variations result in multiple mode changes in flame anchoring and reaction zone orientation, revealing substantial asymmetries over the burner transverse plane. Fig. 8 demonstrates an intermediate stage during the "ramp-up" phase. Both instantaneous and time-averaged chemiluminescence images extracted at Re_D =17x10³ and ϕ =0.9 indicate a heavy bias in heat release towards the right-hand side of the burner axis. As this is a transition stage where vortex breakdown has not been established yet, the flame is not swirl stabilized, but a jet flame partially skewed by the azimuthal momentum provided by the radial (outer swirler).

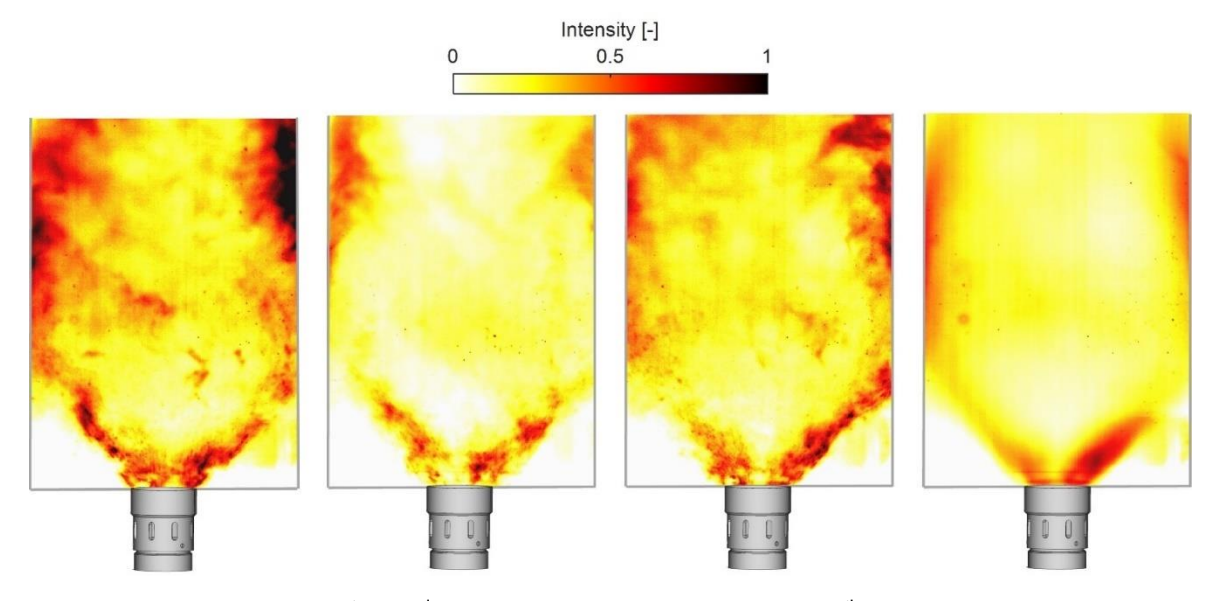


Figure 9 – Instantaneous (1st to 3rd columns) and time-averaged (4th column) chemiluminescence images of confined ethanol/air combustion at Re_D =22x10³ and ϕ =0.84 with pilot methane support using a 30° CW inner swirler.

Once air mass flow rate values above 18 g/s are reached, vortex breakdown is confirmed, and swirl stabilization fully controls the flame dynamics. Hence, to ensure stable conditions after the final mode change of the flame shape, the air mass flow rate is set to 20 g/s, which corresponds to Re_D =22x10³ for the given air temperature. After reaching the aimed operating condition, the pilot methane support is deemed down to zero to stabilize the flame purely on ethanol fuel supply. At these conditions, the vortex breakdown results in a V-shaped flame with the reaction zone closely located to the burner exit. Stronger axial velocity at an increased air mass flow rate also causes the outer recirculation zones (ORZ) to increase the apex angle of the swirl cone, aiding the flame anchoring closer to the burner exit. Although the fuel mass flow rate is also increased at higher air mass flow rates, the elevated azimuthal momentum induced by the radial swirler promotes better break-up fuel droplets. The increased thermal load contributes to the facilitated evaporation of liquid fuel upon injection, and the elevated Reynolds number enhances the mixing of fuel with air. These factors combined a confined reaction zone in proximity to the burner compared to lower Re number operation and significantly improved the azimuthal symmetry of the flame (Fig.9).

3.2 Numerical Results

Fig. 7 presents instantaneous snapshots taken from the LES for Jet A. The circumferential velocity contours show the strong swirl motion induced by the TARS in such a co-rotating configuration, which develops along the whole domain towards the outlet. The basic feature of the turbulent flow structures is captured, with large to medium scales of vortices and even smaller ones depicted early within the inner swirler. The fuel mass fraction indicates where the fuel evaporates, is transported in the swirling turbulent flow, and is consumed due to reaction. Once the liquid fuels were injected within the outer swirler channel, small fuel droplets evaporate quickly forming gaseous fuels. The fuel stream is transported towards the sidewall due to swirling flow motion and chemical reactions take place once the fuel gas is mixed with ambient air, forming a diffusion flame. The reaction zone of this diffusion flame can be associated with the zones of high heat release rates. A relatively thin and thickened Mstructured flame is predicted in the simulations. The presence of the fuel along the outer shear layer and the absence of air cooling from the bottom plate prevents quenching the outer part of the flame, leading to a flame attachment to the TARS nozzle. This flame structure was also observed in the same burner under unconfined flame experiments operated with ethanol, Fig. 7. The more usual and expected V-shaped flame is predicted on the inner side, which sits under the CRZ, strongly dominating the outer recirculation zones in the flame front within the inner channel. bottom corners of the confinement chamber. Consequently, the temperature distribution shows how the strong swirl opens the flame cone and how the hot gases recirculate in the CRZ and slightly penetrate within the inner swirler channel. The negative axial velocity is significant here, coupled with the turbulent structures generated by the inner swirler vanes, which results in an axial translation in the time of the flame front within the inner channel.

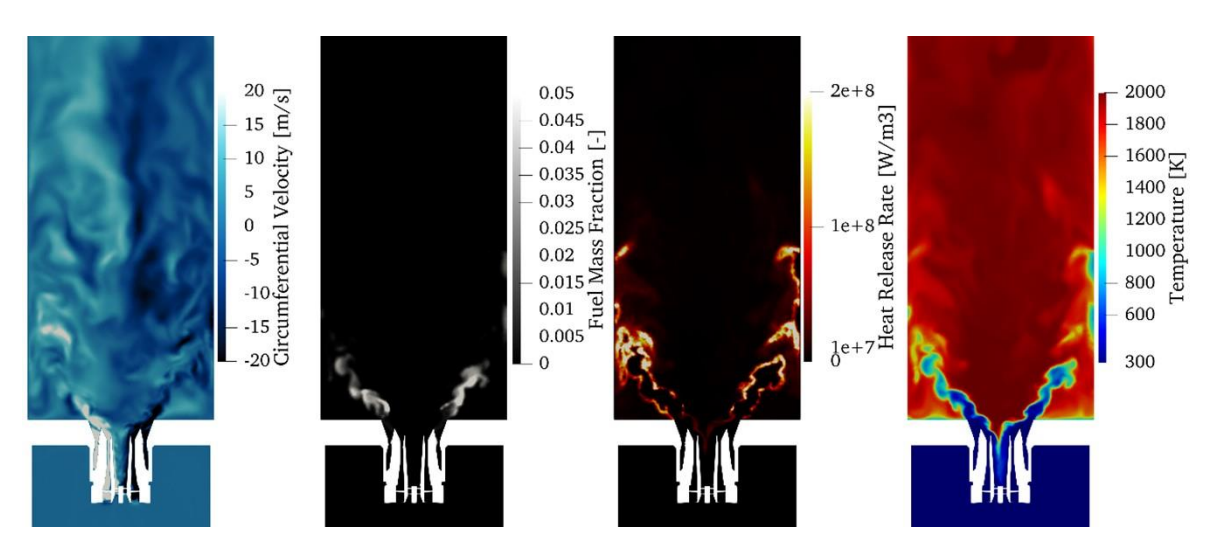


Figure 10 – Instantaneous reactive LES snapshots: azimuthal velocity, fuel mass fraction, heat release rate and temperature distribution obtained for Jet A (from left to right).

Fig. 8 shows time-averaged contours of the LES results obtained for Jet A and ATJ C1. Even though the global behavior is very similar in both cases where the gaseous fuel is distributed along the outer swirl flow, it is found that Jet A is oxidized slightly faster than ATJ C1 after evaporation. One of the potential factors is the liquid penetration length of the fuels. ATJ C1 penetrates slightly further than Jet A, as indicated in LES. As a result, the kerosene-grade Jet A burns more intensely and closer to the TARS nozzle compared to ATJ C1, which shows a more diffuse and less intense heat release distribution along the M-shaped flame.

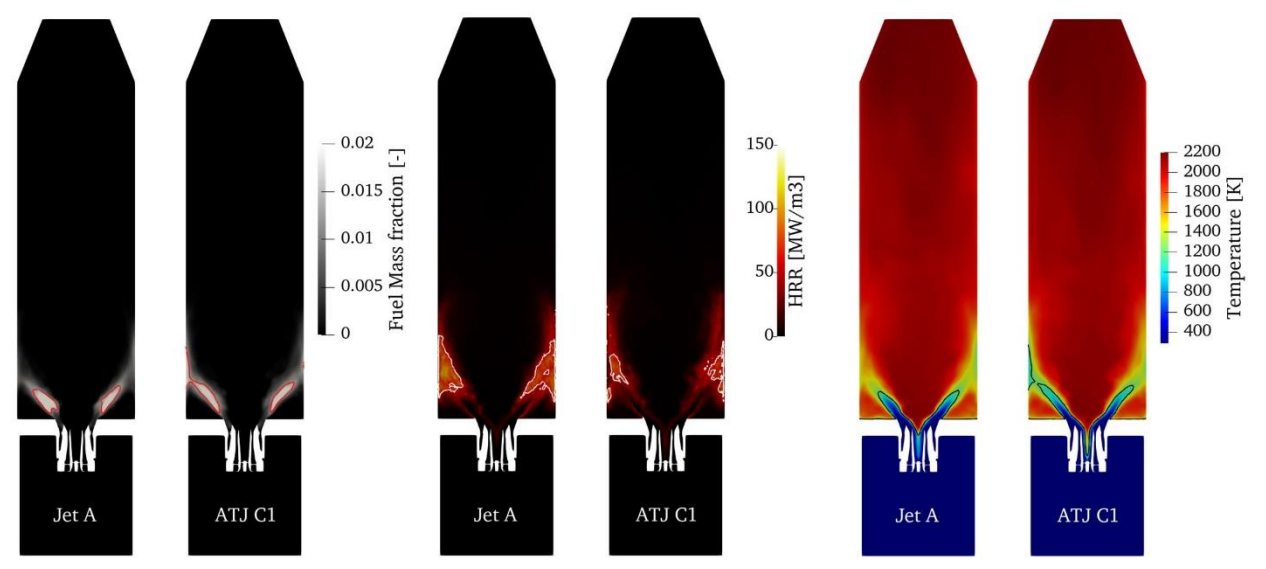


Figure 11 – Time-averaged reactive LES results: fuel mass fractions with contour line for Y_{Fuel} = 0.015 (left), heat release rates with contour line for HRR = 60 MW/m3 (middle) and temperature distributions with contour line for T = 1150 K (right) obtained for Jet A and ATJ C1 using the Z79 class of mechanisms.

4. Conclusions

Stringent requirements for achieving lower global emission levels in aviation demand alternative fuels to be developed for improved sustainability, for which jet fuels of biological origin are accepted as a feasible solution. This necessitates the characterization of thermochemical properties and combustion characteristics before their utilization can be made widespread. Accordingly, the Triple Annular Research Swirler (TARS) burner, which simulates aeroengines combustors, is employed for experimental and numerical investigations of non-reactive and reactive flow dynamics in atmospheric combustion chamber conditions.

Experimental investigations were comprised of two fuel injection schemes (gaseous and liquid), two swirler combination configurations (no inner swirler and 30° CW inner swirler) and two boundary conditions (unconfined and confined). The gaseous fuel tests were conducted utilizing methane (CH₄) as the fuel source and a maximum of Re_D =16x10³ is reached in unconfined combustion conditions for which no inner swirler is mounted in the burner. Although an axisymmetric flame behavior is observed within the range of operating conditions tested, the mass flow limitations through the fuel injection holes restricted gaseous fuel operation to lower thermal loads. Proceeding the gaseous fuel tests, liquid fuel tests are started with ethanol (C_2H_6O) as the fuel source. With the addition of a counter rotating (30° CW) inner swirler into the burner assembly, swirl stabilized non-premixed combustion is established using lean direct injection (LDI) of ethanol. Both for unconfined and confined configurations, it is shown that a sufficiently large mass flow rate of air and a corresponding large thermal load is required for establishing vortex breakdown. Under confined conditions, the operational boundary for symmetric swirl-stabilized combustion is confirmed to be shifted towards lower Reynolds numbers and thermal loads with the combined contribution of outer recirculation zones, prevention of air entrainment and spillage of fuel.

The numerical simulation campaign performed with Large Eddy Simulations focused on investigations at higher Reynolds numbers and thermal loads in comparison to the measurements using Jet A and

ATJ C1. Since the simulations are utilized as a preliminary assessment tool for the combustion characteristics, conditions that are not tested experimentally are investigated. Accordingly, not only fuel type and operating conditions differ from the experimental settings, but also the effects of a corotating inner swirler (30° CCW inner swirler) are analyzed. Despite the different fuel type, operating range and swirler configuration are different than the ones used in the experiments (ethanol), the flame behavior is captured with significantly good agreement with the experimental data provided in terms of chemiluminescence images. This is further utilized in the design of experiment studies to identify the realizable testing range and the targeted operating conditions for kerosene-based jet fuel tests.

5. Future Work

The commissioning campaign of the TARS burner for investigation of alternative jet fuels is still ongoing. The milestones presented in this paper are being followed by an extensive exploration of the operational envelope of the burner using liquid fuels. In this regard, the combined experimental and numerical campaigns will serve as a unique database for understanding the interactions between flow physics and thermochemical processes that take place for swirl-stabilized flames. The experimental data acquired throughout the measurement campaign will be used as a reference for validation and comparison purposes, to investigate the influence of various numerical schemes and modelling approaches employed for the simulation campaigns. Accordingly, the TARS burner will be utilized to characterize fuel injection, flow and flame interaction, and combustion characteristics of various bio grade jet fuels. The kerosene-based jet fuel Jet-A, and alcohol-to-jet biofuel, C1, are to be used as baseline cases for the identification of characteristic differences between different fuels.

Acknowledgements

This project has received funding from the European Union's Horizon 2020 research and innovation programme, MORE & LESS (MDO and REgulations for Low-boom and Environmentally Sustainable Supersonic aviation) project under grant agreement No 101006856, the CESTAP (Competence cEntre in Sustainable Turbine fuels for Aviation and Power) supported by the Swedish Energy Agency, industry and academia in collaboration. Computer time was provided by the Swedish National Infrastructure for Computing (SNIC), partially funded by the Swedish Research Council through grant agreement No 218-05973.

Copyright Statement

The authors confirm that they, and/or their company or organization, hold copyright on all of the original material included in this paper. The authors also confirm that they have obtained permission, from the copyright holder of any third-party material included in this paper, to publish it as part of their paper. The authors confirm that they give permission or have obtained permission from the copyright holder of this paper, for the publication and distribution of this paper as part of the ICAS proceedings or as individual off-prints from the proceedings.

References

- [1] J. Hoelzen, D. Silberhorn, T. Zill, B. Bensmann and R. Hanke-Rauschenbach, "Hydrogen-powered aviation and its reliance on green hydrogen infrastructure Review and research gaps," *International Journal of Hydrogen Energy*, vol. 47, no. 5, pp. 3108-3130, 2022.
- [2] T. K. Hari, Z. Yaakob and N. N. Binitha, "Aviation biofuel from renewable resources: Routes, opportunities and challenges," *Renewable and Sustainable Energy Reviews*, vol. 42, pp. 1234-1244, 2015.
- [3] C. K. Westbrook, "Biofuels Combustion," *Annual Review of Physical Chemistry*, vol. 64, no. 1, pp. 201-219, 2013.
- [4] J. M. Bergthorson and Murray J. Thomson, "A review of the combustion and emissions properties of advanced transportation biofuels and their impact on existing and future engines," *Renewable and Sustainable Energy Reviews*, vol. 42, pp. 1393-1417, 2015.
- [5] E. J. Gutmark, S. Verfaillie, J.-P. Bonnet and F. Grinstein, "Linear Stochastic Estimation of a Swirling Jet," *AIAA JOURNAL*, 2006.

- [6] C. O. Umeh, Z. Rusak and R. V. D. J. C. Ephraim Gutmark, "Experimental and Computational Study of Non-Reacting Vortex Breakdown in a Swirl-Stabilized Combustor," in *47th AIAA Aerospace Sciences Meeting Including The New Horizons Forum and Aerospace Exposition*, 2009.
- [7] P. Iudiciani, C. Duwig, S. M. Hosseini, R. Z. Szasz, L. Fuchs and E. J. Gutmark, "Proper Orthogonal Decomposition for Experimental Investigation of Flame Instabilities," *AIAA JOURNAL*, vol. 50, no. 9, 2012.
- [8] P. Iudiciani, E. J. Gutmark, S. M. Hosseini, R. Collin, A. Lantz, R.-Z. Szász, C. Duwig, L. Fuchs and M. Aldén, "Characterization of a multi-swirler fuel injector using simultaneous laser based planar measurements of reaction zone, flow field and fuel distribution," *Proceedings Of The Asme Turbo Expo 2009*, vol. 2, pp. 1041-1052, 2009.
- [9] C. O. U. Umeh, Z. Rusak and E. J. Gutmark, "Experimental Study of Reaction and Vortex Breakdown in a Swirl-Stabilized Combustor," in *Proceedings of ASME Turbo Expo 2009: Power for Land, Sea and Air*, 2009.
- [10] H. Li, X. Zhou, J. B. Jeffries and R. K. Hanson, "Active control of lean blowout in a swirl-stabilized combustor using a tunable diode laser," *Proceedings of the Combustion Institute*, vol. 31, no. 2, pp. 3215-3223, 2007.
- [11] R. V. Gomez, S. Murugappan, E. Gutmark and C. O. U. Umeh, "Characterization and Dynamics of Lean Direct Injection Swirl-Stabilized Flames," in *45th AIAA/ASME/SAE/ASEE Joint Propulsion Conference & Exhibit*, 2009.
- [12] F. F. Grinstein, T. R. Young, E. J. Gutmark, G. Li, G. Hsiao and H. C. Mongia, "Flow dynamics in a swirl combustor," *Journal of Turbulence*, vol. 3, no. 1, 2002.
- [13] C. Fureby, F. Grinstein, G. Li and E. Gutmark, "An experimental and computational study of a multi-swirl gas turbine combustor," *Proceedings of the Combustion Institute*, vol. 31, no. 2, pp. 3107-3114, 2007.
- [14] P. Iudiciani, C. Duwig, S. M. Hosseini, R. Szasz, L. Fuch and E. Gutmark, "LES investigation and sensitivity analysis of the flow dynamics in a gas turbine swirl combustor," in *49th AIAA Aerospace Sciences Meeting including the New Horizons Forum and Aerospace Exposition*, 2011.
- [15] H. G. Weller, G. Tabor, H. Jasak and C. Fureby, "A tensorial approach to computational continuum mechanics using object-oriented techniques," *Computers in Physics,* vol. 12, no. 6, p. :620–631, 1998.
- [16] L. Lucchese, "Implementation of non-reflecting boundary conditions in OpenFOAM," in *In Proceedings of CFD with OpenSource Software*, 2022.
- [17] J. T. Edwards, "Reference Jet Fuels for Combustion Testing," in *55th AIAA Aerospace Sciences Meeting*, Grapevine, Texas, 2017.
- [18] S. Menon and C. Fureby, "Computational Combustion," *Encyclopedia of Aerospace Engineering*, 2010.
- [19] W.-W. Kim and S. Menon, "A new dynamic one-equation subgrid-scale model for large eddy simulations," in *33rd Aerospace Sciences Meeting and Exhibit*, Reno,NV,U.S.A., 1995.
- [20] V. Sabelnikov and C. Fureby, "LES combustion modeling for high Re flames using a multiphase analogy," *Combustion and Flame*, vol. 160, no. 1, pp. 83-96, 2013.
- [21] N. Zettervall, C. Fureby and E. J. K. Nilsson, "Small Skeletal Kinetic Mechanism for Kerosene Combustion," *Energy Fuels*, vol. 30, no. 11, p. 9801–9813, 2016.